Decentralized Active Damping of Rotating Positioning Platforms

T. Dehaeze [1,3], **C. Collette** [1,2]
[1] Precision Mechatronics Laboratory
University of Liege, Belgium

[2] BEAMS Department
Free University of Brussels, Belgium

[3] European Synchrotron Radiation Facility
Grenoble, France e-mail: **thomas.dehaeze@esrf.fr**

Abstract
Abstract text to be done

1 Introduction

Controller Poles are shown by black crosses (✖). Due to gyroscopic effects, the guaranteed robustness properties of Integral Force Feedback do not hold. Either the control architecture can be slightly modfied or mechanical changes in the system can be performed. This paper has been published The Matlab code that was use to obtain the results are available in [1].

2 Dynamics of Rotating Positioning Platforms

2.1 Studied Rotating Positioning Platform

Consider the rotating X-Y stage of Figure 1.

- k: Actuator's Stiffness [N/m]
- m: Payload's mass [kg]
- $\Omega = \dot{\theta}$: rotation speed [rad/s]
- F_u, F_v
- d_u, d_v

2.2 Equations of Motion

The system has two degrees of freedom and is thus fully described by the generalized coordinates $[q_1 \ q_2] = [d_u \ d_v]$ (describing the position of the mass in the rotating frame).

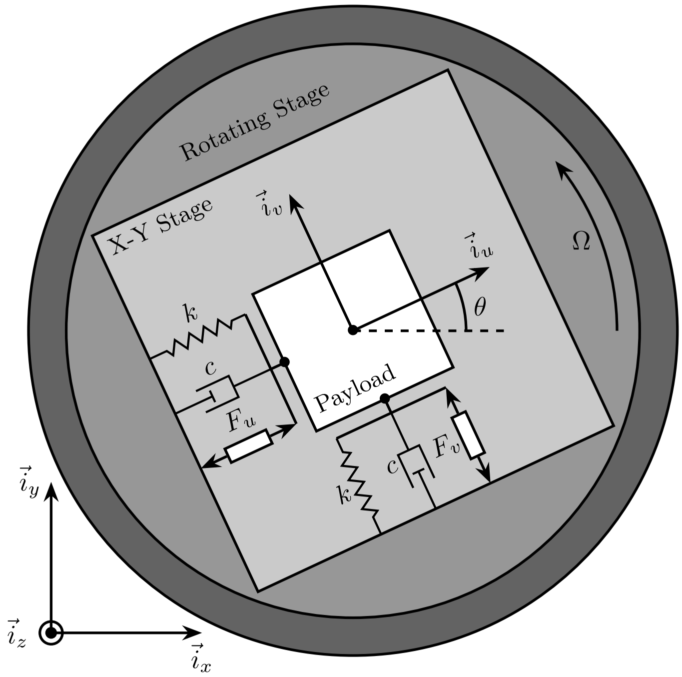

Figure 1: Schematic of the studied System

Let's express the kinetic energy T, the potential energy V of the mass m (neglecting the rotational energy) as well as the deceptive function R:

$$T = \frac{1}{2} m \left(\left(\dot{d}_u - \Omega d_v \right)^2 + \left(\dot{d}_v + \Omega d_u \right)^2 \right) \tag{1a}$$

$$V = \frac{1}{2} k \left({d_u}^2 + {d_v}^2 \right) \tag{1b}$$

$$R = \frac{1}{2} c \left({\dot{d}_u}^2 + {\dot{d}_v}^2 \right) \tag{1c}$$

The equations of motion are derived from the Lagrangian equation:

$$\frac{d}{dt} \left(\frac{\partial L}{\partial \dot{q}_i} \right) + \frac{\partial D}{\partial \dot{q}_i} - \frac{\partial L}{\partial q_i} = Q_i \tag{2}$$

with $L = T - V$ is the Lagrangian and Q_i is the generalized force associated with the generalized variable q_i ($Q_1 = F_u$ and $Q_2 = F_v$).

$$m\ddot{d}_u + c\dot{d}_u + (k - m\Omega) d_u = F_u + 2m\Omega\dot{d}_v \tag{3a}$$

$$m\ddot{d}_v + c\dot{d}_v + (k \underbrace{- m\Omega}_{\text{Centrif.}}) d_v = F_v \underbrace{- 2m\Omega\dot{d}_u}_{\text{Coriolis}} \tag{3b}$$

The Gyroscopic effects can be seen from the two following terms:

- Coriolis Forces: coupling
- Centrifugal forces: negative stiffness

2.3 Transfer Functions in the Laplace domain

Using the Laplace transformation on the equations of motion (3), the transfer functions from $[F_u,\ F_v]$ to $[d_u,\ d_v]$ are obtained:

$$d_u = \frac{ms^2 + cs + k - m\Omega^2}{\left(ms^2 + cs + k - m\Omega^2\right)^2 + \left(2m\Omega s\right)^2} F_u + \frac{2m\Omega s}{\left(ms^2 + cs + k - m\Omega^2\right)^2 + \left(2m\Omega s\right)^2} F_v \tag{4a}$$

$$d_v = \frac{-2m\Omega s}{\left(ms^2 + cs + k - m\Omega^2\right)^2 + \left(2m\Omega s\right)^2} F_u + \frac{ms^2 + cs + k - m\Omega^2}{\left(ms^2 + cs + k - m\Omega^2\right)^2 + \left(2m\Omega s\right)^2} F_v \tag{4b}$$

Without rotation $\Omega = 0$ and the system corresponds to two uncoupled one degree of freedom mass-spring-damper systems:

$$d_u = \frac{1}{ms^2 + cs + k} F_u \tag{5a}$$

$$d_v = \frac{1}{ms^2 + cs + k} F_v \tag{5b}$$

2.4 Change of Variables / Parameters for the study

In order this study is more independent on the system parameters, the following change of variable is performed:

- $\omega_0 = \sqrt{\frac{k}{m}}$: Natural frequency of the mass-spring system in $\mathrm{rad/s}$
- $\xi = \frac{c}{2\sqrt{km}}$: Damping ratio

$$\begin{bmatrix} d_u \\ d_v \end{bmatrix} = \boldsymbol{G}_d \begin{bmatrix} F_u \\ F_v \end{bmatrix} \tag{6}$$

Where $\boldsymbol{G}_d$ is a 2×2 transfer function matrix.

$$\boldsymbol{G}_d = \frac{1}{k} \frac{1}{G_{dp}} \begin{bmatrix} G_{dz} & G_{dc} \\ -G_{dc} & G_{dz} \end{bmatrix} \tag{7}$$

With:

$$G_{dp} = \left(\frac{s^2}{{\omega_0}^2} + 2\xi \frac{s}{\omega_0} + 1 - \frac{\Omega^2}{{\omega_0}^2} \right)^2 + \left(2 \frac{\Omega}{\omega_0} \frac{s}{\omega_0} \right)^2 \tag{8a}$$

$$G_{dz} = \frac{s^2}{{\omega_0}^2} + 2\xi \frac{s}{\omega_0} + 1 - \frac{\Omega^2}{{\omega_0}^2} \tag{8b}$$

$$G_{dc} = 2 \frac{\Omega}{\omega_0} \frac{s}{\omega_0} \tag{8c}$$

G_{dp} describes to poles of the system, G_{dz} the zeros of the diagonal terms and G_{dc} the coupling.

- $k = 1\,\mathrm{N/m}$, $m = 1\,\mathrm{kg}$, $c = 0.05\,\mathrm{N\,m^{-1}\,s}$
- $\omega_0 = 1\,\mathrm{rad\,s^{-1}}$, $\xi = 0.025$

2.5 System Dynamics and Campbell Diagram

The bode plot of $\boldsymbol{G}_d$ is shown in Figure 2.

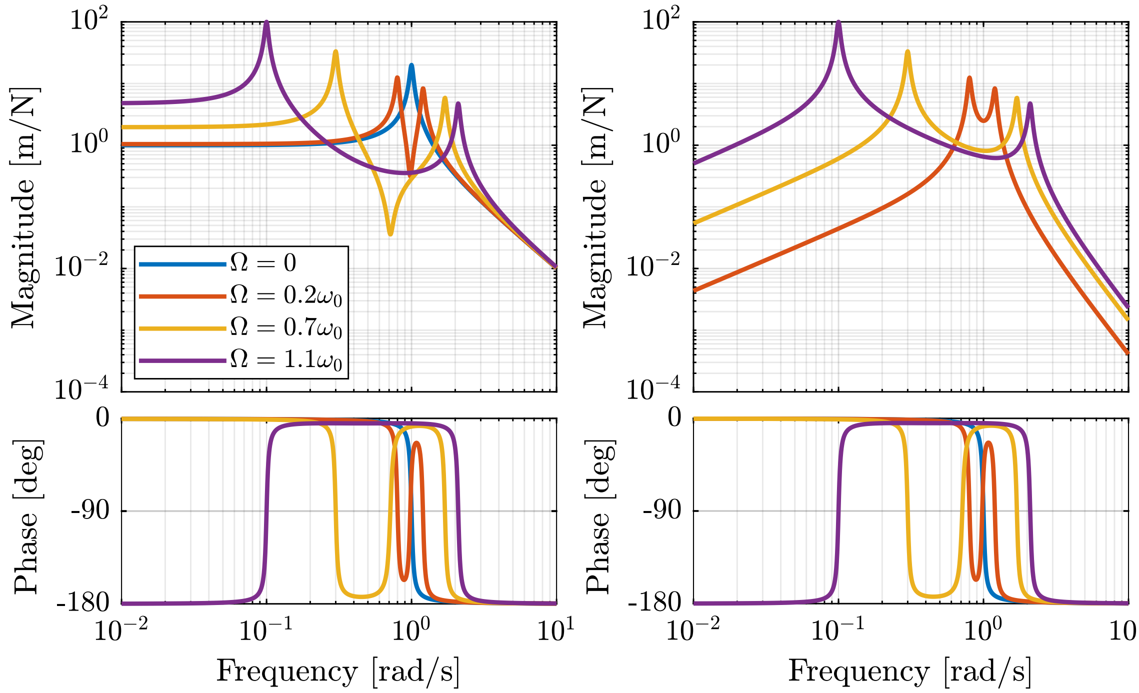

(a) Direct Terms d_u/F_u, d_v/F_v

(b) Coupling Terms d_v/F_u, d_u/F_v

Figure 2: Bode Plots for $\boldsymbol{G}_d$

The poles are the roots of G_{dp}. Two pairs of complex conjugate poles (supposing small damping $\xi \approx 0$):

$$p_1 = \pm j(\omega_0 - \Omega) \tag{9a}$$

$$p_2 = \pm j(\omega_0 + \Omega) \tag{9b}$$

When the rotation speed in non-null, the resonance frequency is split into two pairs of complex conjugate poles. As the rotation speed increases, one of the two resonant frequency goes to lower frequencies as the other one goes to higher frequencies.

When the rotational speed Ω reaches ω_0, the real part of one pair of complex conjugate becomes position meaning is system is unstable.

The stiffness of the X-Y stage is too small to hold to rotating payload hence the instability.

Stiff positioning platforms should be used if high rotational speeds or heavy payloads are used.

3 Decentralized Integral Force Feedback

3.1 System Schematic and Control Architecture

Force Sensors are added in series with the actuators as shown in Figure 4.

3.2 Plant Dynamics

The forces measured by the force sensors are equal to:

$$\begin{bmatrix} f_u \\ f_v \end{bmatrix} = \begin{bmatrix} F_u \\ F_v \end{bmatrix} - (cs + k) \begin{bmatrix} d_u \\ d_v \end{bmatrix} \tag{10}$$

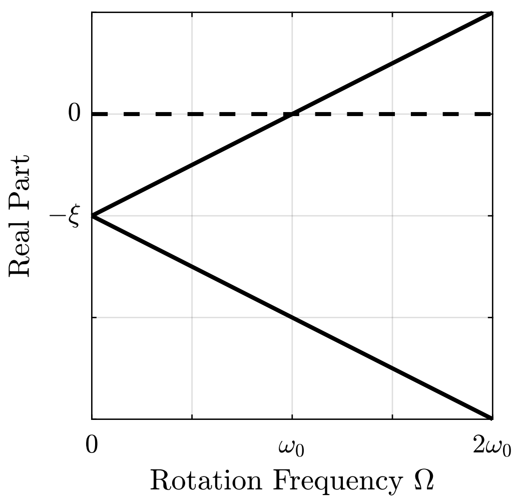

(a) Real Part

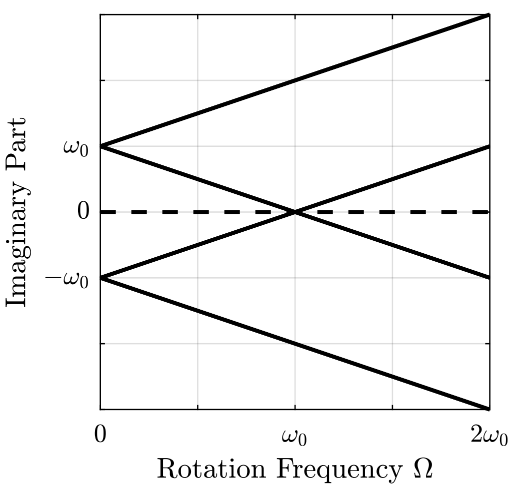

(b) Imaginary Part

Figure 3: Campbell Diagram : Evolution of the poles as a function of the rotational speed Ω

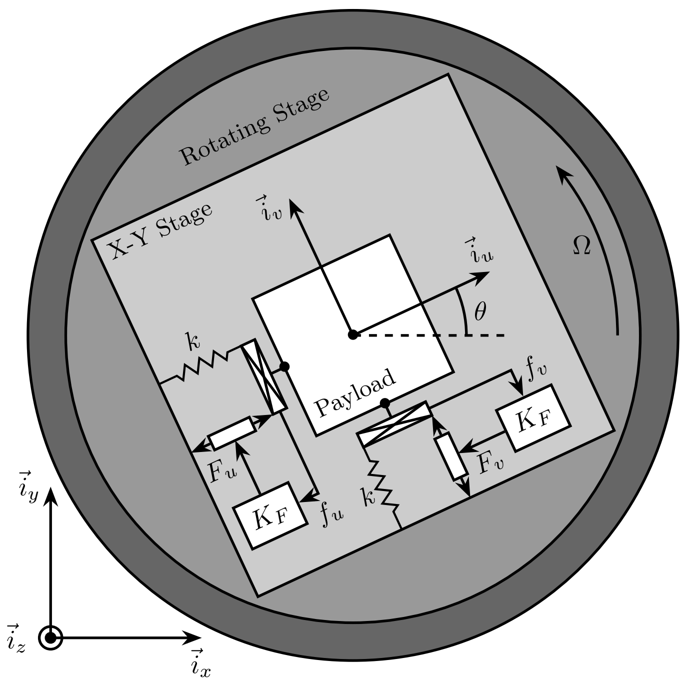

Figure 4: System with Force Sensors in Series with the Actuators. Decentralized Integral Force Feedback is used

Re-injecting (6) into (10) yields:

$$\begin{bmatrix} f_u \\ f_v \end{bmatrix} = \boldsymbol{G}_f \begin{bmatrix} F_u \\ F_v \end{bmatrix} \tag{11}$$

Where $\boldsymbol{G}_f$ is a 2×2 transfer function matrix.

$$\boldsymbol{G}_f = \frac{1}{G_{fp}} \begin{bmatrix} G_{fz} & -G_{fc} \\ G_{fc} & G_{fz} \end{bmatrix} \tag{12}$$

with:

$$G_{fp} = \left(\frac{s^2}{{\omega_0}^2} + 2\xi \frac{s}{\omega_0} + 1 - \frac{\Omega^2}{{\omega_0}^2} \right)^2 + \left(2 \frac{\Omega}{\omega_0} \frac{s}{\omega_0} \right)^2 \tag{13}$$

$$G_{fz} = \left(\frac{s^2}{{\omega_0}^2} - \frac{\Omega^2}{{\omega_0}^2} \right) \left(\frac{s^2}{{\omega_0}^2} + 2\xi \frac{s}{\omega_0} + 1 - \frac{\Omega^2}{{\omega_0}^2} \right) + \left(2 \frac{\Omega}{\omega_0} \frac{s}{\omega_0} \right)^2 \tag{14}$$

$$G_{fc} = \left(2\xi \frac{s}{\omega_0} + 1 \right) \left(2 \frac{\Omega}{\omega_0} \frac{s}{\omega_0} \right) \tag{15}$$

The zeros of the diagonal terms are the roots of G_{fz} (supposing small damping):

$$z_1 = \pm j \omega_0 \sqrt{\frac{1}{2} \sqrt{8 \frac{\Omega^2}{{\omega_0}^2} + 1} + \frac{\Omega^2}{{\omega_0}^2} + \frac{1}{2}} \tag{16a}$$

$$z_2 = \pm \omega_0 \sqrt{\frac{1}{2} \sqrt{8 \frac{\Omega^2}{{\omega_0}^2} + 1} - \frac{\Omega^2}{{\omega_0}^2} - \frac{1}{2}} \tag{16b}$$

The frequency of the two complex conjugate zeros z_1 is between the frequency of the two pairs of complex conjugate poles p_1 and p_2. This is the expected behavior of a collocated pair of actuator and sensor.

However, the two real zeros z_2 induces an increase of +2 of the slope without change of phase (Figure 5). This represents non-minimum phase behavior.

The low frequency gain, for $\Omega < \omega_0$, is no longer zero:

$$\boldsymbol{G}_{f0} = \lim_{\omega \to 0} |\boldsymbol{G}_f(j\omega)| = \begin{bmatrix} \frac{-\Omega^2}{{\omega_0}^2 - \Omega^2} & 0 \\ 0 & \frac{-\Omega^2}{{\omega_0}^2 - \Omega^2} \end{bmatrix} \tag{17}$$

It increase with the rotational speed Ω.

3.3 Decentralized Integral Force Feedback

$$\boldsymbol{K}_F(s) = g \cdot \frac{1}{s} \tag{18}$$

Also, as one zero has a positive real part, the **IFF control is no more unconditionally stable**. This is due to the fact that the zeros of the plant are the poles of the closed loop system with an infinite gain. Thus, for some finite IFF gain, one pole will have a positive real part and the system will be unstable.

At low frequency, the gain is very large and thus no force is transmitted between the payload and the rotating stage. This means that at low frequency, the system is decoupled (the force sensor removed) and thus the system is unstable.

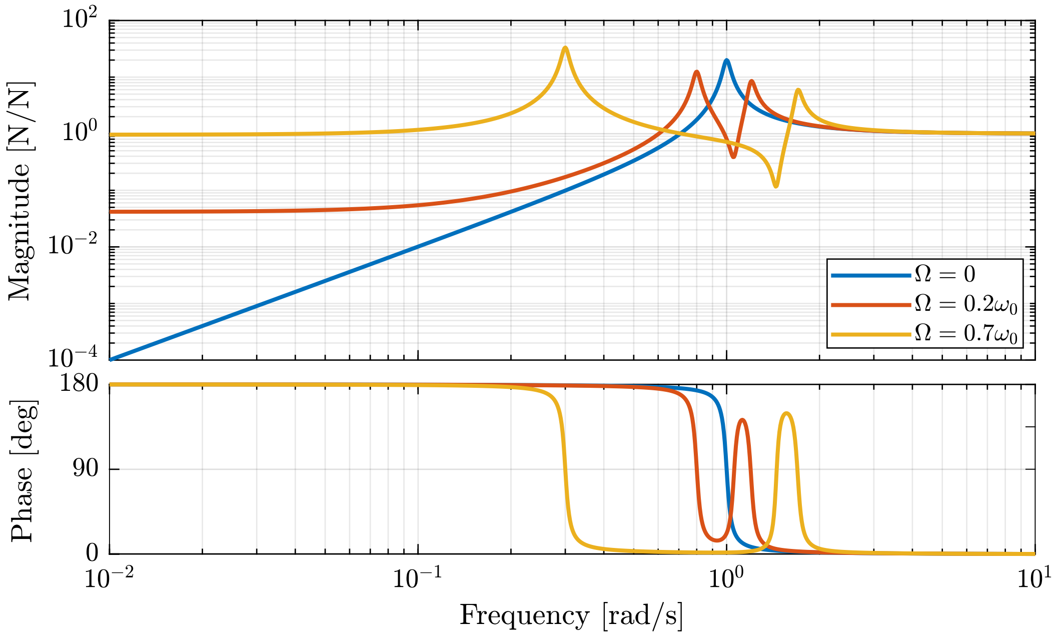

Figure 5: Bode plot of $\boldsymbol{G}_f$ for several rotational speeds Ω

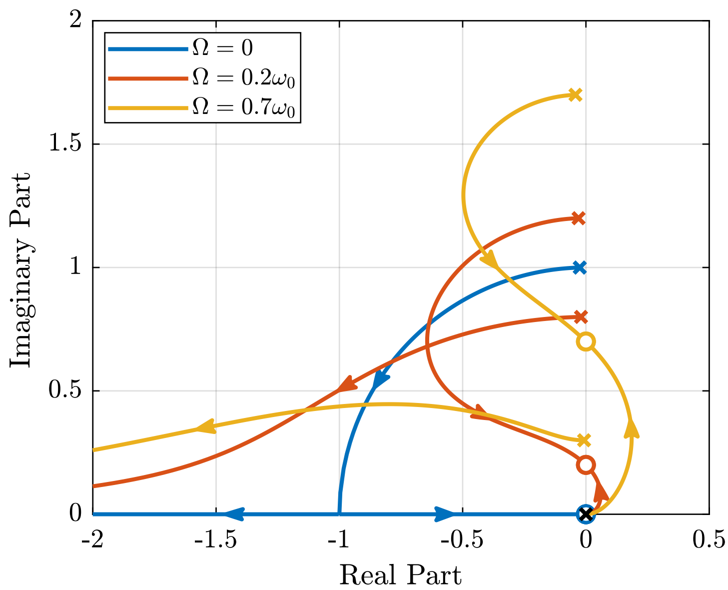

Figure 6: Root Locus for the Decentralized Integral Force Feedback

4 Integral Force Feedback with High Pass Filters

4.1 Modification of the Control Low

$$\boldsymbol{K}_F(s) = g \cdot \frac{1}{s} \cdot \underbrace{\frac{s/\omega_i}{1 + s/\omega_i}}_{\text{HPF}} = g \cdot \frac{1}{s + \omega_i} \tag{19}$$

4.2 Feedback Analysis

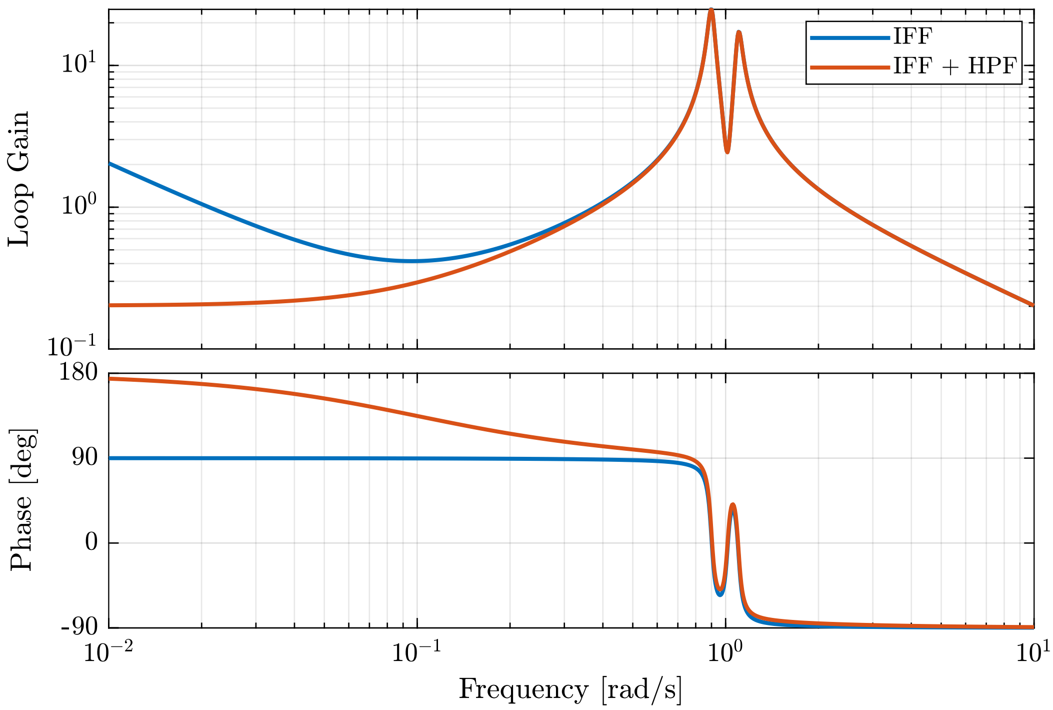

Figure 7: Bode Plot of the Loop Gain for IFF with and without the HPF

$$g_{\text{max}} = \omega_i \left(\frac{{\omega_0}^2}{\Omega^2} - 1 \right) \tag{20}$$

4.3 Optimal Cut-Off Frequency

5 Integral Force Feedback with Parallel Springs

5.1 Stiffness in Parallel with the Force Sensor

5.2 Plant Dynamics

We define an adimensional parameter α, $0 \leq \alpha < 1$, that describes the proportion of the stiffness in parallel with the actuator and force sensor:

$$k_p = \alpha k \tag{21a}$$
$$k_a = (1 - \alpha) k \tag{21b}$$

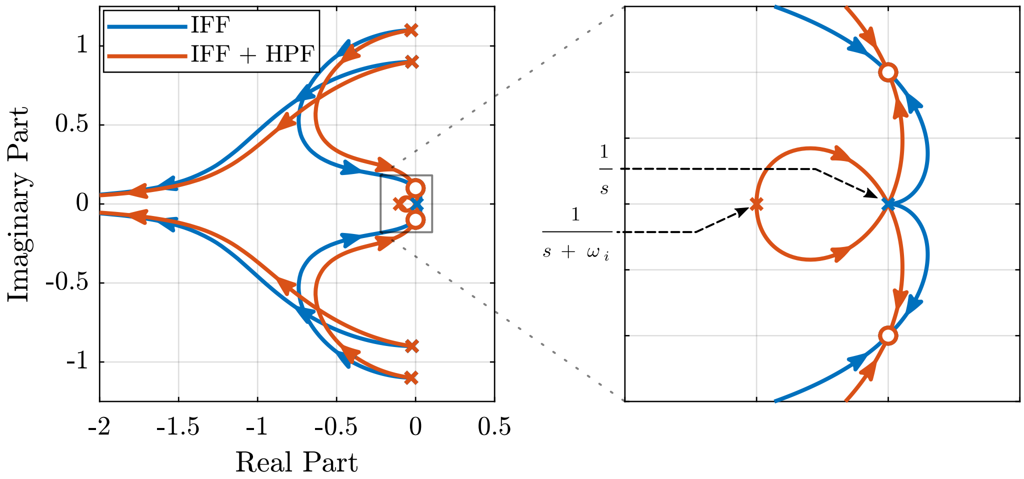

Figure 8: Root Locus for IFF with and without the HPF

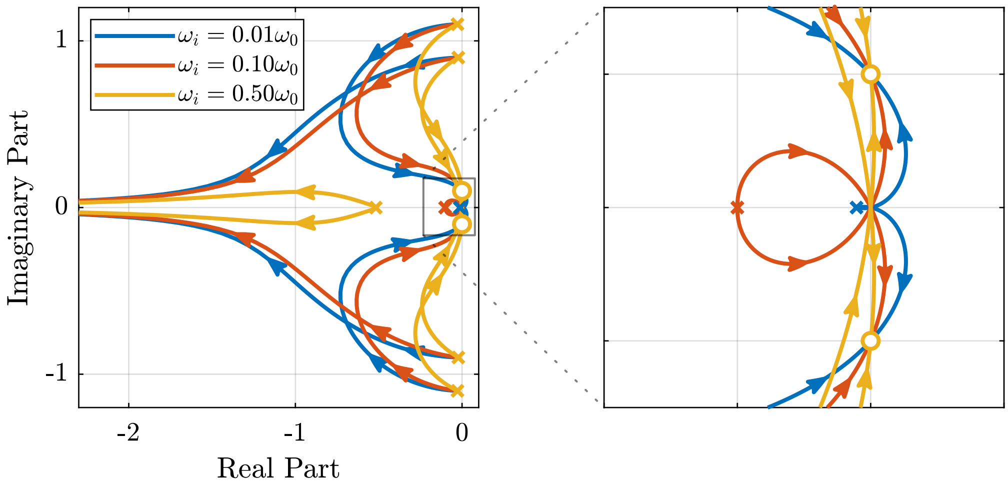

Figure 9: Root Locus for several HPF cut-off frequencies ω_i

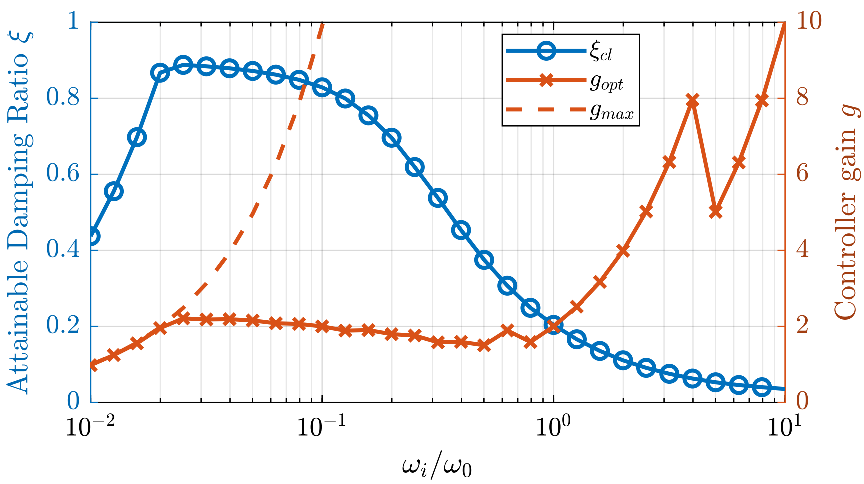

Figure 10: Attainable damping ratio ξ_{cl} as a function of the HPF cut-off frequency. Corresponding control gain g_{opt} and g_{max} are also shown

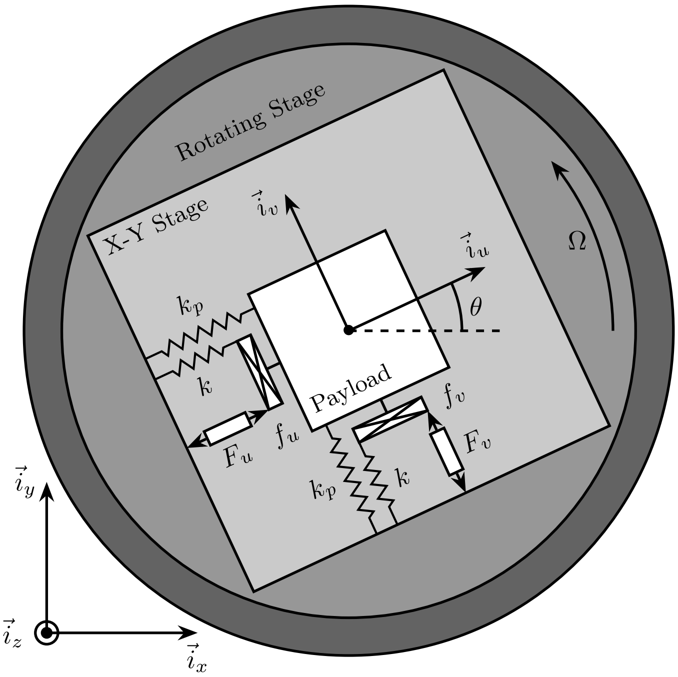

Figure 11: System with added springs in parallel with the actuators

The overall stiffness k stays constant:

$$k = k_a + k_p \tag{22}$$

$$\begin{bmatrix} f_u \\ f_v \end{bmatrix} = \boldsymbol{G}_k \begin{bmatrix} F_u \\ F_v \end{bmatrix} \tag{23}$$

$$\begin{bmatrix} f_u \\ f_v \end{bmatrix} = \frac{1}{G_{kp}} \begin{bmatrix} G_{kz} & -G_{kc} \\ G_{kc} & G_{kz} \end{bmatrix} \begin{bmatrix} F_u \\ F_v \end{bmatrix} \tag{24}$$

With:

$$G_{kp} = \left(\frac{s^2}{{\omega_0}^2} + 2\xi \frac{s}{\omega_0} + 1 - \frac{\Omega^2}{{\omega_0}^2} \right)^2 + \left(2 \frac{\Omega}{\omega_0} \frac{s}{\omega_0} \right)^2 \tag{25a}$$

$$G_{kz} = \left(\frac{s^2}{{\omega_0}^2} - \frac{\Omega^2}{{\omega_0}^2} + \alpha \right) \left(\frac{s^2}{{\omega_0}^2} + 2\xi \frac{s}{\omega_0} + 1 - \frac{\Omega^2}{{\omega_0}^2} \right) + \left(2 \frac{\Omega}{\omega_0} \frac{s}{\omega_0} \right)^2 \tag{25b}$$

$$G_{kc} = \left(2\xi \frac{s}{\omega_0} + 1 - \alpha \right) \left(2 \frac{\Omega}{\omega_0} \frac{s}{\omega_0} \right) \tag{25c}$$

5.3 Effect of the Parallel Stiffness on the Plant Dynamics

$$\begin{aligned} \alpha &> \frac{\Omega^2}{{\omega_0}^2} \\ \Leftrightarrow k_p &> m\Omega^2 \end{aligned} \tag{26}$$

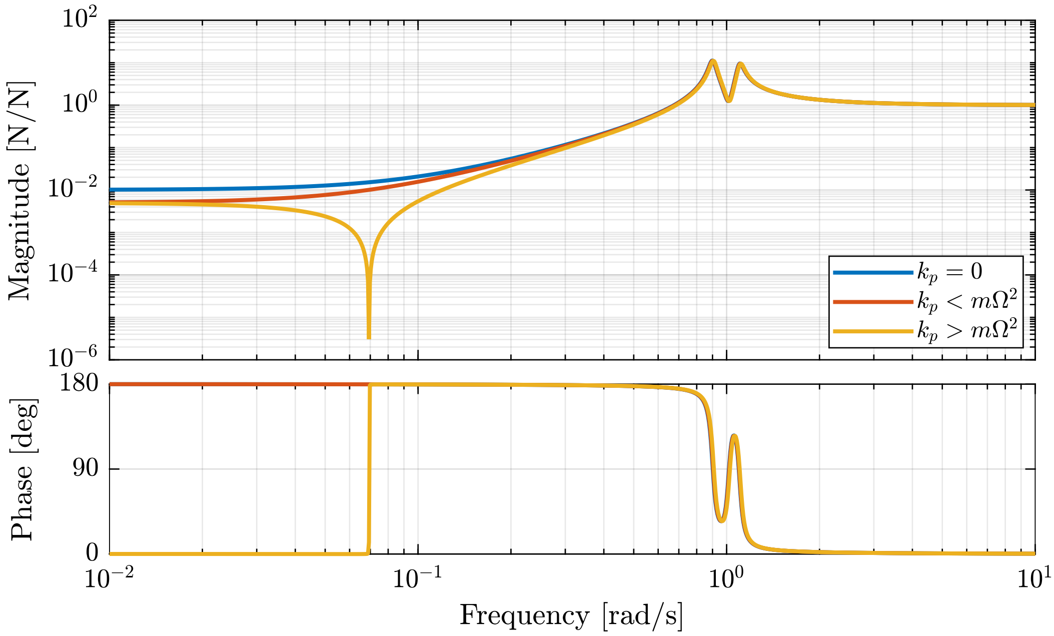

Figure 12: Bode Plot of f_u/F_u without parallel spring, with parallel springs with stiffness $k_p < m\Omega^2$ and $k_p > m\Omega^2$

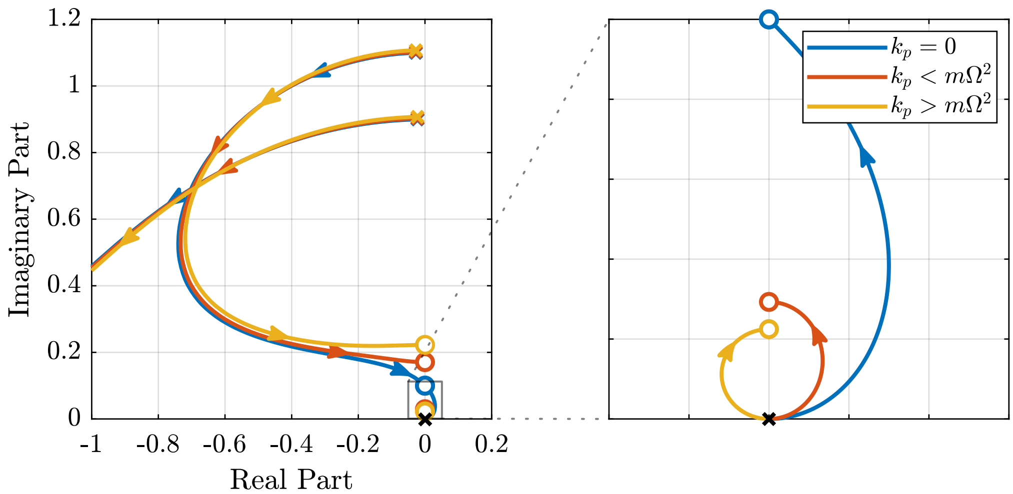

Figure 13: Root Locus for IFF without parallel spring, with parallel springs with stiffness $k_p < m\Omega^2$ and $k_p > m\Omega^2$

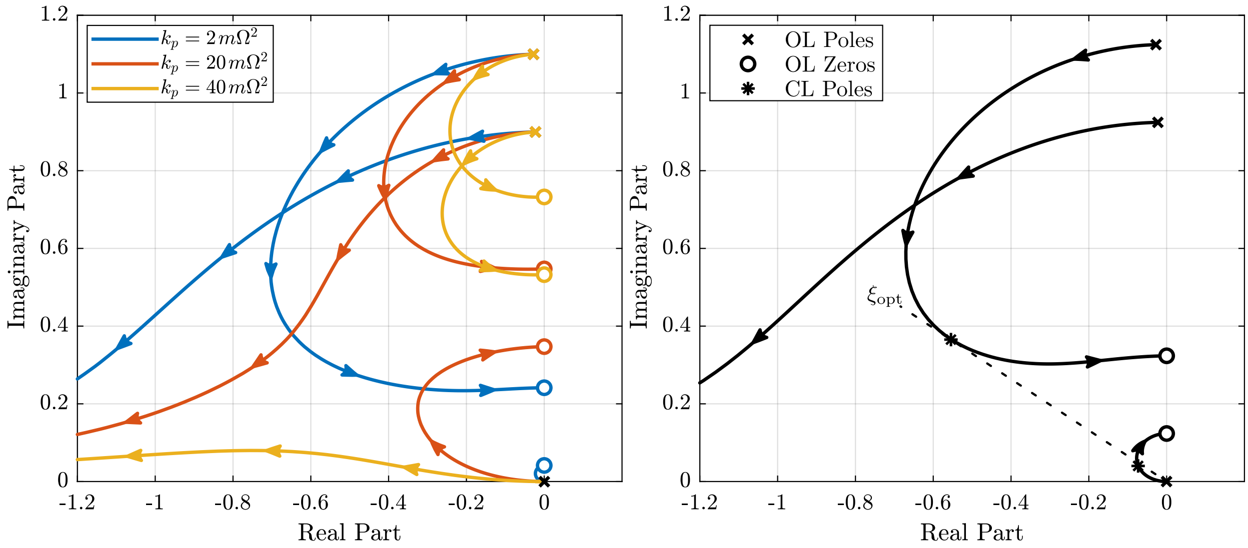

(a) Three values of k_p (b) $k_p = 5m\Omega^2$, optimal damping is shown

Figure 14: Root Locus for IFF when parallel stiffness is used

5.4 Optimal Parallel Stiffness

6 Direct Velocity Feedback

6.1 System Schematic and Control Architecture

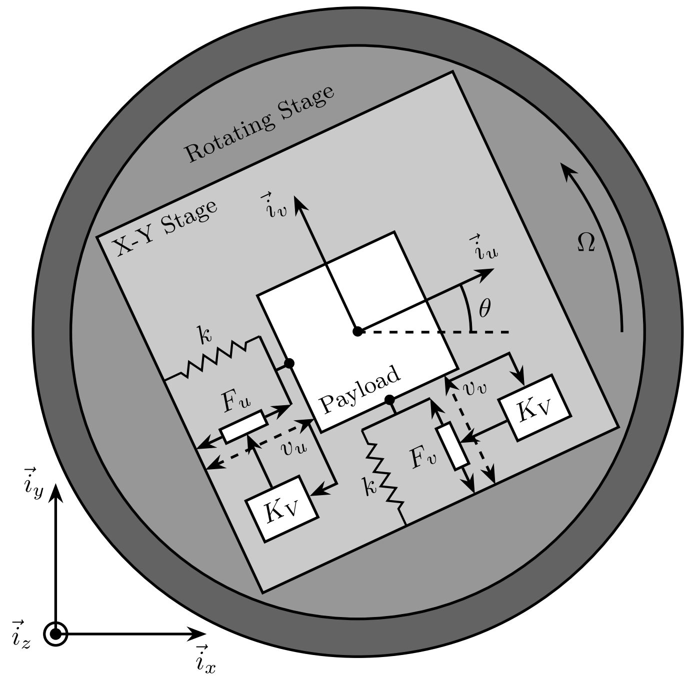

Figure 15: System with relative velocity sensors and with decentralized controllers K_V

6.2 Equations

$$\begin{bmatrix} v_u \\ v_v \end{bmatrix} = \boldsymbol{G}_v \begin{bmatrix} F_u \\ F_v \end{bmatrix} \tag{27}$$

$$\begin{bmatrix} v_u \\ v_v \end{bmatrix} = \frac{1}{k} \frac{1}{G_{vp}} \begin{bmatrix} G_{vz} & G_{vc} \\ -G_{vc} & G_{vz} \end{bmatrix} \begin{bmatrix} F_u \\ F_v \end{bmatrix} \tag{28}$$

With:

$$G_{vp} = \left(\frac{s^2}{{\omega_0}^2} + 2\xi \frac{s}{\omega_0} + 1 - \frac{\Omega^2}{{\omega_0}^2} \right)^2 + \left(2 \frac{\Omega}{\omega_0} \frac{s}{\omega_0} \right)^2 \tag{29a}$$

$$G_{vz} = s \left(\frac{s^2}{{\omega_0}^2} + 2\xi \frac{s}{\omega_0} + 1 - \frac{\Omega^2}{{\omega_0}^2} \right) \tag{29b}$$

$$G_{vc} = 2 \frac{\Omega}{\omega_0} \frac{s}{\omega_0} \tag{29c}$$

6.3 Relative Direct Velocity Feedback

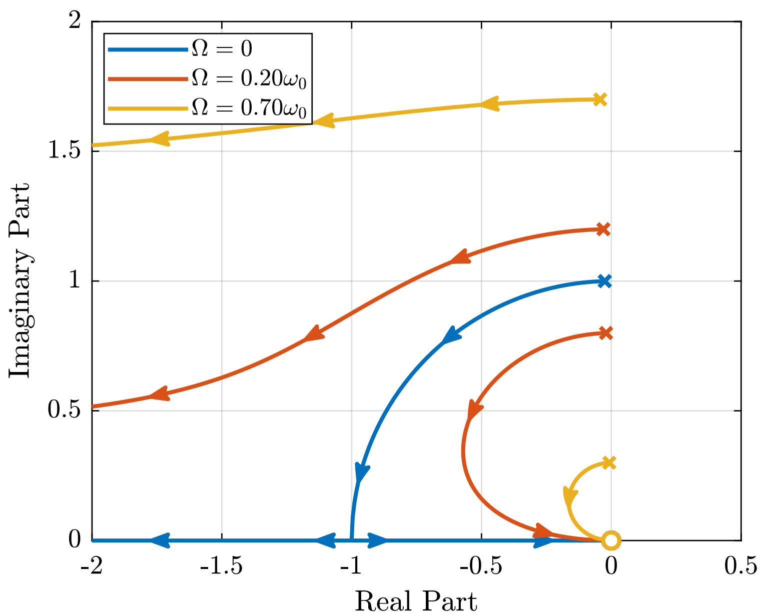

Figure 16: Root Locus for Decentralized Direct Velocity Feedback for several rotational speeds Ω

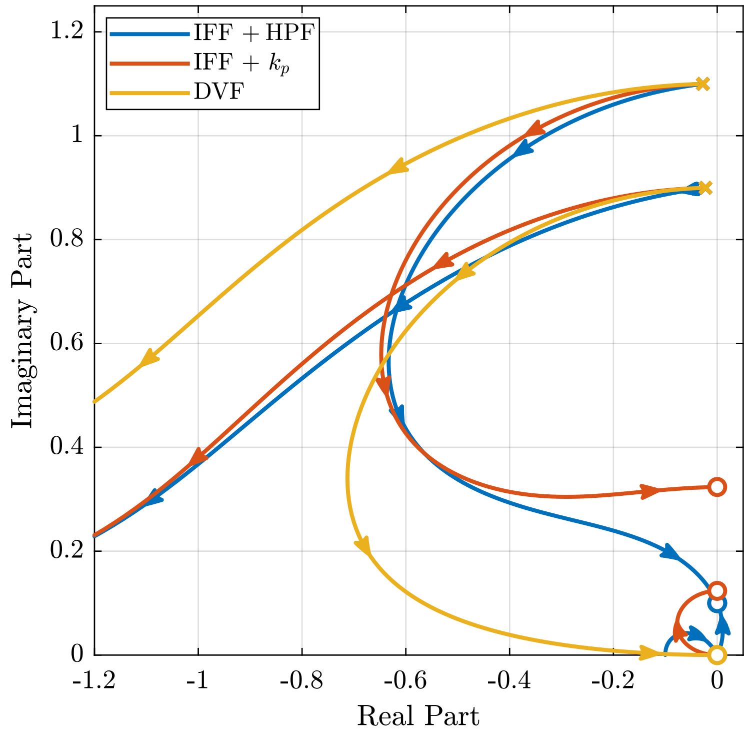

Figure 17: Root Locus for the three proposed decentralized active damping techniques: IFF with HFP, IFF with parallel springs, and relative DVF

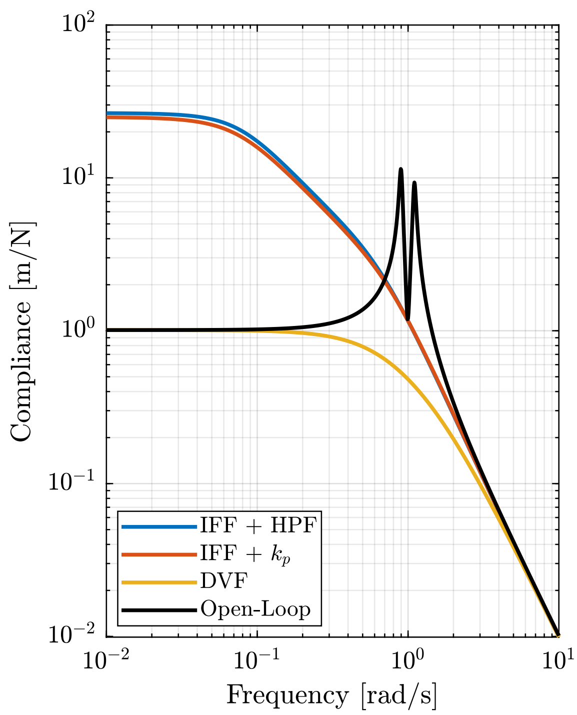

(a) Transmissibility

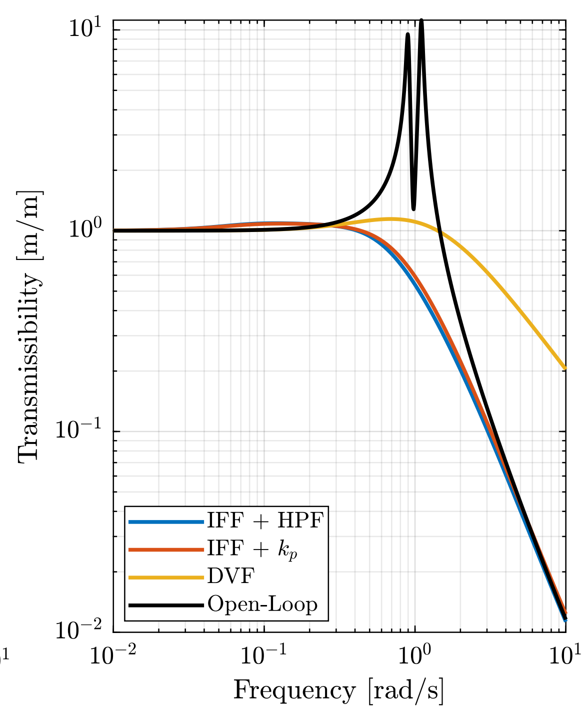

(b) Compliance

Figure 18: Comparison of the three proposed Active Damping Techniques

7 Comparison of the Proposed Active Damping Techniques for Rotating Positioning Stages

7.1 Physical Comparison

7.2 Attainable Damping

7.3 Transmissibility and Compliance

8 Conclusion

Acknowledgment

References

[1] T. Dehaeze, "Active damping of rotating positioning platforms," Source Code on Zonodo, 07 2020. [Online]. Available: https://doi.org/10.5281/zenodo.3894342